

# Tape casting of nanocrystalline ceria gadolinia powder

Lorenz P. Meier<sup>a,\*</sup>, Lukas Urech<sup>a</sup>, Ludwig J. Gauckler<sup>b</sup>

<sup>a</sup> Riedtlistr. 67, 8006 Zurich, Switzerland

<sup>b</sup> Nonmetallic Materials, Swiss Federal Institute of Technology, Switzerland

Received 30 April 2003; received in revised form 16 December 2003; accepted 2 January 2004

Available online 10 May 2004

## Abstract

A ceramic ceria gadolinia solid solution membrane for solid oxide fuel cells was fabricated by tape casting using a nanopowder of 37 nm average particle size. A novel combination of solvent and dispersant was used to disperse the nanoparticles. The polymer was added in a dilute stage to guarantee a homogeneous distribution. After casting a remarkable densification of the cast tape suspension from a solid loading of 20 up to 42 vol.% was observed during drying. The green tape was sintered to >92% theoretical density and was dense towards perfusion. The resulting grain size in the sintered specimen still was <200 nm.

© 2004 Elsevier Ltd. All rights reserved.

*Keywords:* Tape casting; CeO<sub>2</sub>; Fuel cell; Nanoparticles

## 1. Introduction

### 1.1. Ceria gadolinia electrolyte for solid oxide fuel cells

Fuel cells are able to convert the chemical energy of fuel molecules such as hydrogen by oxidation into electrical energy. Alkanes as fuel also can be oxidised but need elevated temperatures to be cleaved as performed in solid oxide fuel cells, SOFC. In case of SOFC one functional part is the electrolyte which is ion conductive for, i.e. O<sup>2-</sup> ions. Apart from the ionic conductivity a basic requirement is the mechanical stability of the electrolyte. Up to now yttria stabilised zirconia (YSZ) is used due to its excellent mechanical properties and ion conductivity. The use of nanometre grain sized gadolinia doped ceria, CGO, is expected to lower the operating temperatures because of its considerably higher O<sup>2-</sup>-ion conductivity.<sup>1–7</sup> For both reasons, mechanical strength and high ionic conductivity, the use of CGO requires the sintered ceramic electrolyte to have a grain size well below 1 μm. Thus, nano-sized powders have to be used.

### 1.2. Nanopowders processing

Nanocrystalline dense ceramics promise several advantages compared to standard ceramics, but they are difficult

to achieve. To fully densify the ceramic body during sintering, the solid loading of the green body needs to be as high as possible. However, colloiddally stable nano-sized powder suspensions are known to have a markedly lower volume loading compared to suspensions with larger particle sizes.<sup>8</sup> When the particles are sterically stabilised by dispersing molecules, an adhering layer of these molecules on the surface in the order of a few nanometres is generated (Fig. 1).<sup>9</sup> For particle sizes larger than 100 nm the volume loss can be neglected. With decreasing size of the particles, the adhering layer becomes more and more important. For particles in the nanometre range, it becomes significant and the maximum volume loading for a stable suspension is decisively lower. As a consequence of this, the green bodies resulting from nanopowders usually have low green densities and are difficult to sinter to dense ceramics.<sup>10,11</sup>

### 1.3. Tape casting

Tape casting is a convenient shaping method to produce two-dimensional thin ceramic plates of usually 10–1000 μm thickness.<sup>8,12,13</sup> A paste-like suspension consisting of powder, organic solvent, dispersant, polymer (binder) and plasticiser is cast onto a substrate by a moving blade in a constant distance to the substrate. The final dried green tape is flexible, not sensitive to mechanical stresses and thus, easy to handle. This processing method as well as the equip-

\* Corresponding author.

E-mail address: [lorenz@meier.name](mailto:lorenz@meier.name) (L.P. Meier).

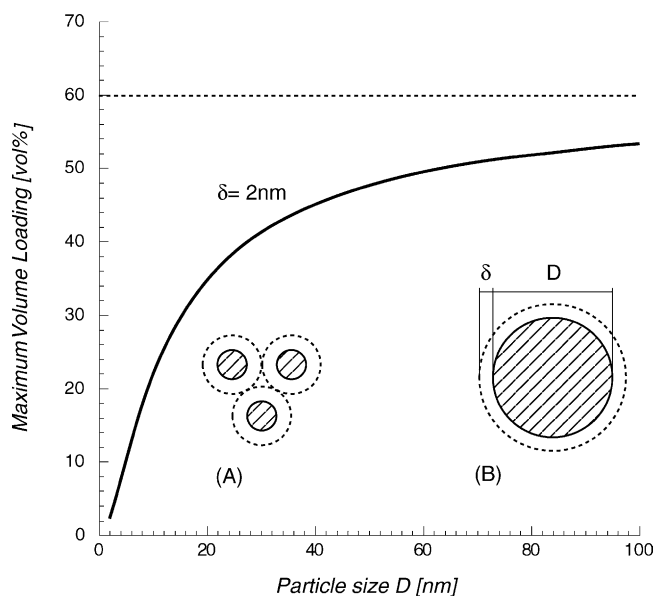


Fig. 1. The volume of the stabilising dispersant layer (here  $\delta = 2$  nm) becomes more and more important for smaller radii. It influences the maximum achievable volume loading (usually around 60 vol.%). Whereas for larger particles (B) this lost volume is negligible, it becomes more and more considerable for small particles (A).

ment is simple and therefore is interesting for many types of applications such as dielectrics for capacitors, chip carrier substrates and sensor supports.<sup>13</sup>

One of the main challenges in tape casting is to formulate a suitable suspension composition as many kinds of cracks may arise during drying. Generally, the suspension has a solid loading of >40 vol.% to avoid pronounced shrinkage of the particle network during drying.<sup>8,14–16</sup> Ceramic powders with a mean particle size in the range of 0.5–2  $\mu\text{m}$  are typically used and just few attempts have been reported using smaller particles. In tape casting literature, alumina powders with 0.12  $\mu\text{m}$  mean particle sizes (surface of >12  $\text{m}^2/\text{g}$ ) are already considered as high surface area powders.<sup>13</sup> Although many dispersants and solvent systems are proposed,<sup>17–26</sup> very few tape casting reports exist where grain sizes <100 nm have been used.<sup>27</sup>

We report a suitable approach to produce a dense ceramic electrolyte for SOFC application by tape casting using an organic solvent as dispersion medium and nano-sized  $\text{Ce}_{0.9}\text{Gd}_{0.1}\text{O}_{1.95}$  (CGO) powder of 37 nm particle size. A novel dispersant and solvent system has been developed to improve the colloidal stability. The procedure was adapted to the problems with nanopowders.

## 2. Materials and methods

### 2.1. Materials

#### 2.1.1. Ceramic oxide powder

The powder used was  $\text{Ce}_{0.9}\text{Gd}_{0.1}\text{O}_{1.95}$  supplied by Rhodia (Lot 199/273/98). The elemental composition was 89.0

atom%  $\text{CeO}_2$  and 11.0 atom%  $\text{Gd}_2\text{O}_3$ . The mean particle size evaluated by sedimentation was 37 nm (Brookhaven Instruments Corporation, XDC centrifuge sedigraph), which is in good agreement with the mean particle size derived from BET measurements of 24  $\text{m}^2/\text{g}$  (Quantachrome Nova 1000).

It is noteworthy, that processing problems of nanopowder are related to the particle size rather than the surface. The BET surface area of 24  $\text{m}^2/\text{g}$  (=170  $\text{m}^2/\text{ml}$ ) with a high specific density of 7.2 g/ml is comparable in specific surface to an alumina powder (3.98 g/ml) with 43.2  $\text{m}^2/\text{g}$  (24 g/ml alumina = 96  $\text{m}^2/\text{ml}$ ) surface area for the same particle size.

#### 2.1.2. Compounds

The following chemicals used in these experiments were purchased from FLUKA: ethanol (puriss. p.a.), butyl acetate (purum), ethyl acetate (puriss. p.a.), *p*-xylene (purum), Span 80 (sorbitan monooleate), bis(2-ethylhexyl) phthalate (purum) and polyethylene glycol (pract.). Fish oil from menhaden, FOM (“Menhaden fish oil”), was achieved from Sigma. Polyvinyl butanal as the binder polymer was available by Aldrich and cobalt (II) nitrate hexahydrate (p.a.), from Merck.

### 2.2. Methods

#### 2.2.1. Surface-doping with 3 atom% $\text{Co}^{28}$

The ceramic CGO powder was surface-doped with 3 atom% cobalt oxide using Co(II) nitrate to enhance the sintering process.

One hundred grams of CGO powder were dispersed by ultrasonication in 200 ml ethanol. 5.05 g of Co(II) nitrate hexahydrate were dissolved in 100 ml ethanol and added to the suspension. The solvent was evaporated in vacuo at 60 °C using a Buchi Rotavapor. The dried powder then was heated up to 350 °C for 2 h where the nitrate decomposes to the oxide. In this process, the colour of CGO turned to a dark grey due to the Co oxide.

#### 2.2.2. Evaluation of the dispersant amount of Span 80 by sedimentation<sup>27</sup>

18.0 g CGO were added to a solution of the specific Span 80 (sorbitan monooleate; wt.% dispersant refers to CGO) in about 15 ml butyl acetate and diluted to a total suspension volume of 25 ml. The sample was cooled in an ice-water bath and ultrasonicated for 5 min. It was afterwards sedimented in a closed graduated cylinder. The height of the sediment was determined as a function of the time.

The results obtained were compared to a suspension composed of 7 wt.% FOM in a mixture of 3 volume parts *p*-xylene and 2 parts ethanol as used in literature.<sup>13</sup>

### 2.3. Tape casting procedure

#### 2.3.1. General preparation of the suspension for 100 g CGO powder for tape casting

7.00 g of sorbitan monooleate (Span 80; specific density: 0.99 g/ml, dispersant) 3.00 g of polyethylene glycol

Table 1  
The composition of the suspension

Powder	Ceria gadolinia	100 g
Solvent	Butyl acetate	32 ml (+10 ml surplus butyl acetate)
Dispersant	Sorbitane monooleate	7.00 g
Plastisizer	Poly-ethyleneglycol 300 + bis(2-ethylhexyl) phtalate	3.00 g + 3.00 g
Binder (polymer)	Poly-vinylbutanal	9.00 g

(molecular weight 300 g/mol, purum, 1.12 g/ml, plasticiser) and 3.00 g bis(2-ethylhexyl) phtalate (0.985 g/ml, plasticiser) were added to 32 ml of butyl acetate (purum, 0.881 g/ml) and 10 ml as a surplus. Seventy-five grams of CGO (7.2 ml/g; dried at 120 °C) were added and the mixture was milled for 5 min using a planetary mill (Retsch planetary ball mill, zirconia container 500 ml, 1 cm zirconia balls). The rest of the powder (25 g) was added in portions of 10 g while milling for 5 min. The final suspension was milled for another 20 min. The suspension had low viscous appearance. 9.00 g polyvinylbutanal (1.083 g/ml, binder polymer) are added in 3 portions and milled for 5 min. The suspension was controlled to ensure that all of the polymer was dissolved otherwise the milling was prolonged for additional 5 min (Table 1).

The suspension was sieved (50 mesh sieve) and the surplus of butyl acetate was slowly removed in vacuo using a Büchi Rotavapor at 60 °C. It is very important, that the evaporation of surplus of butyl acetate is carried out carefully to avoid drying skin or bubble formation during the evaporation.

The suspension was cast onto a silicon coated PET foil. The tape was fabricated using a doctor blade with a slit width of 1 mm at a blade speed of 4 mm/s. Casting was performed in a closed box, diminishing the formation of a drying skin and to slow down the drying.

### 2.3.2. Rheological measurements

Viscoelastic properties of the suspensions and steady shear viscosity at various shear rates are investigated by rheological measurements using a Bohlin stress-controlled rheometer (Model CS-50, Bohlin Instruments, Sweden) equipped with a measuring tool of plate/plate geometry (rough surface, 25 mm plate diameter). The temperature of the sample is controlled by a thermostat water bath and is kept constant at 20 °C.

Oscillatory measurements are performed at a fixed frequency of 1 Hz, varying the applied strain amplitude. From such an amplitude sweep curve, the elastic and viscous modulus was evaluated. Our amplitude sweep experiments are conducted with a gap of 1 mm between the parallel plates.<sup>29</sup>

### 2.3.3. Recycling of the powder

The powder was recycled after the experiments. The organics were burned out at 350 °C for 24 h in an open dish. It was then milled by a planetary mill for 20 min. No significant grain growth or changes of the powder properties are expected, since the same temperature as for the doping procedure was used.

## 2.4. Sintering<sup>28</sup>

The tape was carefully removed from the substrate foil. It was heated up to 500 °C at a heating rate of 30 °C/h and held for 1 h to slowly remove all organic additives. It was then heated up at 30 °C/min. Final sintering was carried out at 940 and 980 °C for 2 h of holding time.

### 2.4.1. Microstructural analysis

SEM pictures of the thin film microstructure were captured using a LEO 1530 field emission SEM, Germany. The samples were coated with 10 nm of Platinum metal.

## 3. Results and discussion

### 3.1. Dispersant and solvent evaluation

For the reasons of processability the colloidal suspension has to be stable before casting. Due to the low stability of gadolinia in water the particles were dispersed in organic solvent. A novel dispersant and solvent combination has been developed to improve the solid loading of the nanoparticles suspension. An excellent dispersing effect for this CGO nanopowder was obtained using sorbitan monooleate (Span 80) as the dispersant and butyl acetate as the solvent. The influence of different amounts of this dispersant was determined after sedimentation procedure thereby forming a percolating self-standing gel network.<sup>27</sup> The optimum amount of dispersing agent provides a minimum sediment height at maximum particle volume loading. Fig. 2 compares the sedimentation behaviour in the presence of different amounts of the dispersant Span 80 (wt.% to CGO) as a function of time. Smallest sediments were obtained with 7 and 9 wt.% Span 80.

These dispersing agent amounts seem high, but are expected. Since the dispersing agent is meant to adsorb on the powders surface, its amount correlates with the size of the surface. The high amount of dispersant found for this nanopowder of 37 nm particle size is explained by the very high surface (around 1 wt.% FOM for 500 nm powder at higher volume loadings).<sup>8</sup> Furthermore, the content is above the theoretically predicted threshold for a percolating network of around 15 vol.%, which points to a stabilising effect of the particles by the dispersant.<sup>33</sup>

The dispersant effect of this combination was compared to a reference suspension with 7 wt.% FOM in a mixture of 3 parts xylene/2 parts ethanol as the solvent, a widely used

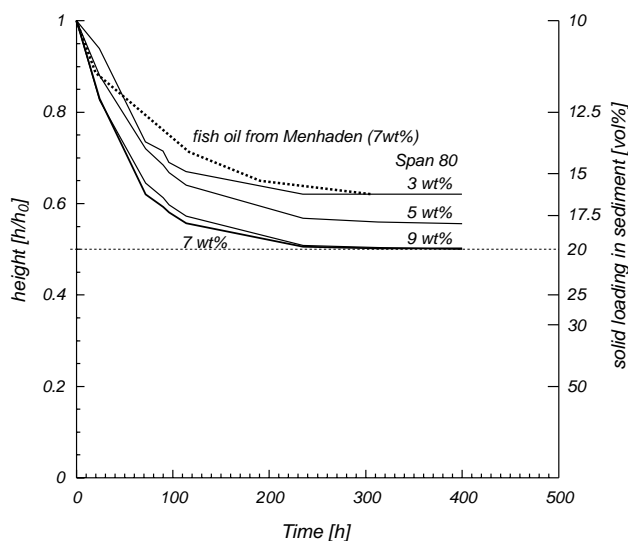


Fig. 2. The dispersant amount for nanometer-sized CGO powder was determined by the sediment volume of a 10 vol.% solid loading suspension. A dispersant amount of >7 wt.% Span 80 in butyl acetate showed highest densification (20 vol.% in sediment). It is compared to FOM (7 wt.%) using a mixture of *p*-xylene/ethanol for which a less efficient dispersing effect has been observed.

system with reported good dispersing effect.<sup>13</sup> However, its dispersing effect for CGO was even smaller than that of the 3 wt.% Span 80 sample and we concluded, that increasing the dispersing agent amount of FOM to clearly above 7 wt.% would significantly lower the suspensions solids content. The sediment of FOM/xylene/ethanol based suspensions clearly does not compact as good as Span 80/butyl acetate and was discarded for further experiments.

As a further advantage of this dispersing system, dispersant and solvent, these compounds are little toxic, i.e. compared to toluene or chlorinated solvents. Span 80 is used as a surfactant in food industries and butyl acetate as solvent and is a natural flavour.

### 3.2. Polymeric binder

The polymer binder system with polyvinyl butanal as the binder and a mixture of polyethyleneglycol and bis(2-ethylhexyl) phthalate as plasticiser is easily soluble in butyl acetate and resulted in reasonably low viscosity suspensions.

The polymer amount was also optimised to obtain an uncracked green tape, which was still flexible after tape casting and drying. The full tape casting procedure was performed and the polymer amount was increased by 33% of the previously chosen amount when cracks have been observed. The polymer to plasticizer composition remained unchanged at a ratio of 3 parts binder polymer/1 part polyethyleneglycol 300/1 part bis(2-ethylhexyl) phthalate.

Too low a polymer content invariably ended in cracked green tapes. We attribute this to the fact, that the particles have to be completely wrapped by the binder polymer and form strictly non-percolating network, which is supported

by the fact, that the tape has the flexible properties of the polymer. Otherwise, a percolating network of the particles with its brittle properties will arise.

### 3.3. Tape casting

#### 3.3.1. Sample preparation and distribution problems

Mixing of the ingredients and the polymer with nanopowders is a serious problem. Performing the suspension preparation with the standard method, where all the ingredients are added to the final amounts, invariably ended in cracked tapes. Therefore, a surplus of solvent was used. The ingredients were mixed in a dilute stage in a planetary mill with the surplus and the surplus was carefully removed before casting. The final tapes were crackfree.

We interpret the results as follows: nanoparticles also generate a nanoporous organic phase for which the diffusion is slowed down by  $1/r^2$  ( $r$ : radius of the pore).<sup>30–32</sup> Since these particles are much smaller than the ones usually used for tape casting, it is a serious task to distribute the polymer homogeneously.

We conclude, that beside a right composition of the suspension, the homogenous distribution of the additives by an improved mixing procedure to be the most important factor for a good tape. A sufficient distribution in nanopowders suspension is guaranteed in the dilute stage followed by careful removal of the solvent surplus.

#### 3.3.2. Rheology of the tape suspension

Rheology measurements on the ready-to-cast suspension was performed. The suspension leads to densely sintered tapes and had a solid content of 20 vol.%. The viscosity was 3 Pa s at a shear rate of  $10 \text{ s}^{-1}$ , 2 Pa s at  $50 \text{ s}^{-1}$  and 1.6 Pa s at  $100 \text{ s}^{-1}$  (Fig. 3). The suspension is regarded as suitable for tape casting.

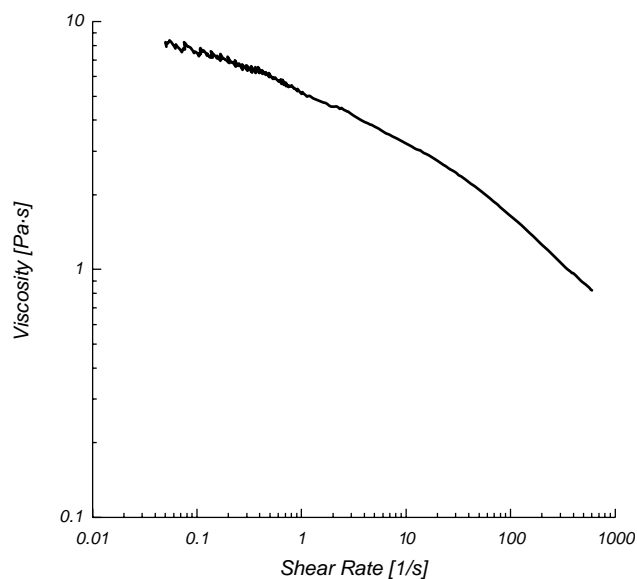


Fig. 3. Viscosity of the suspension with the binder polymer at 25 °C prior casting. (Composition according to Table 1.)

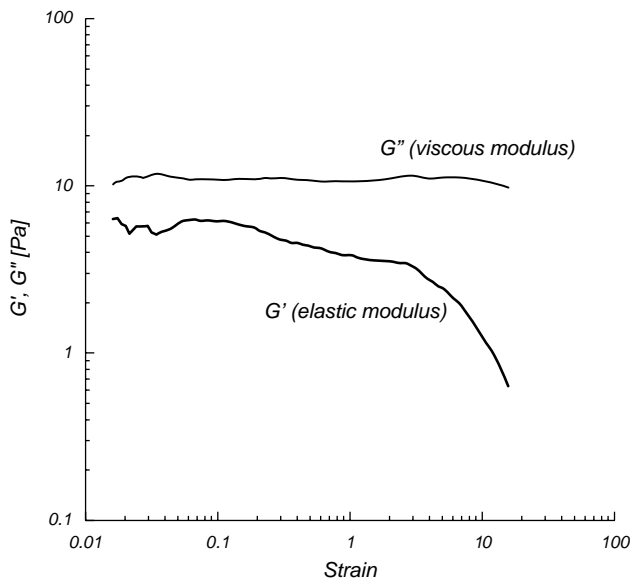


Fig. 4. The viscoelastic properties of the suspension ready for tape casting.

### 3.3.3. Viscoelastic properties of the suspension

In literature, the viscoelastic properties of different tape casting suspensions were discussed and are regarded as important.<sup>8</sup> Therefore, oscillatory measurements of the suspension have been performed and show a predominantly viscous behaviour and low elastic part (Fig. 4).

### 3.4. Drying rate

The influence of the drying rate was investigated using ethyl acetate (boiling point: 77 °C), which also works with the dispersant and polymer system. Best results were found at slow drying rates. Therefore, butyl acetate with a high boiling point of 125 °C is recommended. It allows a good handling without instantaneous formation of a drying skin.

After drying, the tape had a smooth surface and was flexible as requested for well-suited tapes.

### 3.5. Dried tape

After drying for 1–2 days the tape had a green body thickness of 0.22 mm. The specific density of the green tape was 3.60 g/ml as determined by water displacement. The solid loading of the tape is calculated to be about 42 vol.% considering the organic contents and their specific densities.

Even considering the drying shrinkage of more than 50% derived from the increase in volume loading, the thickness of the dry tape (0.22 mm dry refers to about 0.5 mm wet) is smaller than expected from the slit width (1 mm) but is explained by rheological arguments. The moving blade carts parts of a predominantly viscous suspension, which results in a significantly thinner wet and dried tape (theoretically expected for Newtonian liquids: half of the slit width).

### 3.6. Sintering<sup>28</sup>

The green tape was slowly heated up to minimise any destructive influences during burnout. After burning out with a heating rate of 30 °C/h up to 500 °C the sintering was performed at 940 and 980 °C. After sintering at 940 °C the structure still had small pores and was not dense. At 980 °C the structure is dense towards perfusion of liquids like ethanol and acetone. The density increased from 89% of the theoretical density at 940 °C to >92% of the theoretical density at 980 °C of CGO (7.2 g/ml). The thickness of the ceramic tape was 175 μm as determined by SEM.

#### 3.6.1. Microstructure and grain size in the sintered tape

The final ceramic body sintered at 980 °C reached a density of 92% of the theoretical density and was dense to perfusion of solvents such as ethanol. The fracture surface still

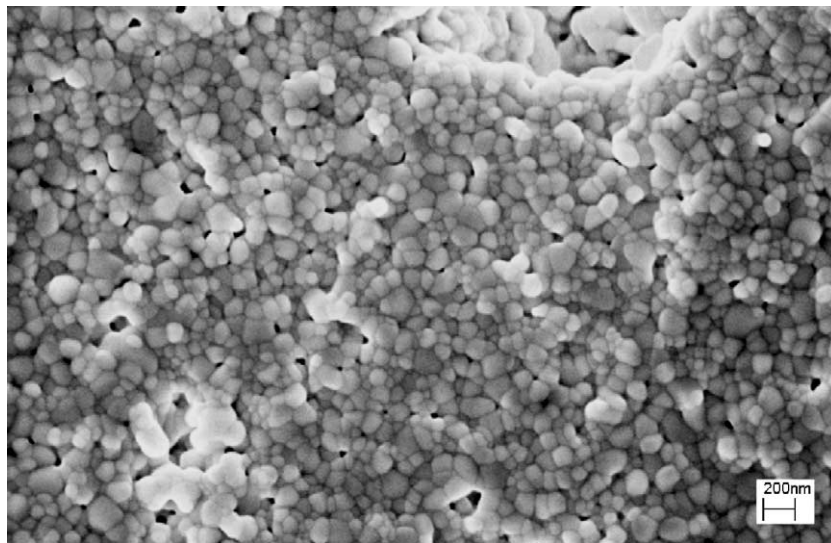


Fig. 5. The surface of a tape sintered at 980 °C. The crystallites were clearly below 200 nm. The surface showed almost no porosity. The body was 175 μm thick and dense towards perfusion of solvents.

showed residual pores. The final grain size was very small <200 nm (Fig. 5), which indicates a very moderate grain growth during the sintering procedure.

#### 4. Conclusions

Tape casting of nanopowders has been successfully carried out. A very good dispersing agent and solvent combination was found. Span 80 as a dispersant and butyl acetate as the solvent were evaluated and the amount was optimised for this nanopowder. The dispersant system showed improved results compared to fish oil from menhaden. Polyvinylbutanal is used as the binder polymer with polyethyleneglycol 300 and bis(2-ethylhexyl) phthalate as plastisizer. The distribution of the additives in nanopowders turned out to be more difficult than in standard powders and it is recommended to use a surplus of solvent, which is then removed by evaporation. The viscoelastic properties of such a suspension are predominantly viscous. Slow drying is important since the low diffusion through the nanoporous suspension leads to a rapid drying skin formation. Considering all these factors a tape suspension was achieved with a solid loading of 20 vol.% which was suitable for to a crackfree tape. The green density of the dry tape was >42 vol.%, which was enough to be sintered a ceramic body dense towards perfusion with 92% theoretical density, while still having a grain size of around 200 nm.

#### Acknowledgements

Our thanks are directed to Dr. E. Tervoort and Dr. A. Studart for discussions and technical support.

#### References

- Gödickemeier, M., Sasaki, K. and Gauckler, L. J., Current–voltage characteristics of fuel cells with ceria–based electrolytes. In *Solid Oxide Fuel Cells IV, Vol 95*, ed. M. Dokiya, O. Yamamoto, H. Tagawa and S. C. Singhal. The Electrochemical Society, Proceedings Series, Pennington, NJ, 1995, pp. 1072–1081.
- Kosacki, I., Suzuki, T., Petrovsky, V. and Anderson, H. U., Electrical conductivity of nanocrystalline ceria and zirconia thin films. *Solid States Ionics* 2000, **136/137**, 1225–1233.
- Riess, I., Gödickemeier, M. and Gauckler, L. J., Characterization of solid oxide fuel cells based on solid electrolytes or mixed ionic electronic conductors. *Solid State Ionics* 1996, **90**, 91–104.
- Schneider, D., Gödickemeier, M. and Gauckler, L. J., Nonstoichiometry and defect chemistry of ceria solid solutions. *J. Electroceram.* 1997, **1**, 165–172.
- Steele, B. C. H., Appraisal of  $Ce(1 - y)Gd(y)O(2 - y/2)$  electrolytes for IT-SOFC operation at 500 °C. *Solid States Ionics* 2000, **129**, 95–110.
- Steele, B. C. H. and Heinzel, A., Materials for fuel-cell technologies. *Nature* 2001, **414**, 345–352.
- Suzuki, T., Kosacki, I. and Anderson, H. U., Electrical conductivity and lattice defects in nanocrystalline cerium oxide thin films. *J. Am. Ceram. Soc.* 2001, **84**, 2007–2014.
- Shanefield, D. J., *Organic Additives and Ceramic Processing: With Applications in Powder Metallurgy, Ink, and Paint*. Kluwer Academic Publishers, Boston, 1995.
- Lewis, J. A., Colloidal processing of ceramics. *J. Am. Ceram. Soc.* 2000, **83**, 2341–2359.
- Colloid Science, Irreversible Systems*, ed. H. R. Kruyt. Elsevier Publishing Company, Amsterdam, 1952.
- Van Herle, J., Oxalate coprecipitation of doped ceria powder for tape casting. *Ceram. Int.* 1998, **24**, 229–241.
- Mistler, R. E., Tape casting: past present potential. *Am. Ceram. Soc. Bull.* 1998, **77**, 82–86.
- Mistler, R. E. and Twiname, E. R., *Tape Casting, Theory and Practice*. American Ceramic Society, 2000.
- Lindquist, K. and Liden, E., Preparation of alumina membranes by tape casting and dip coating. *J. Eur. Ceram. Soc.* 1996, **17**, 356–366.
- Xie, Z.-P., Ma, C., Huang, Y. and Xiang, J., Gel tape casting ceramic sheets. *Am. Ceram. Soc. Bull.* 2002, **81**, 33–37.
- Yu, H. J., Gu, Y. H., Wan, J. L. and Liang, K. M., The preparation of laminated ceramic composites by sedimentation and sieving. *J. Mater. Sci.* 1999, **34**, 2855–2857.
- Brook, R. J., Cahn, R. W., Haasen, P. and Kramer, E. J., *Materials Science and Technology, Vol 17A + 17B. Processing of Ceramics, Part I and Part II*. VCH Verlag, Weinheim, 1996.
- Moreno, R., The role of slip additives in tape-casting technology 1. Solvents and dispersants. *Am. Ceram. Soc. Bull.* 1992, **71**, 1521–1531.
- Moreno, R., The role of slip additives in tape casting technology 2. Binders and plasticizers. *Am. Ceram. Soc. Bull.* 1992, **71**, 1647–1657.
- Moreno, R. and Cordoba, G., Oil dispersion of alumina for tape casting. *Am. Ceram. Soc. Bull.* 1995, **74**, 69–74.
- Moreno, R. and Cordoba, G., Oil-related deflocculants for tape casting slips. *J. Eur. Ceram. Soc.* 1997, **17**, 351–357.
- Nelson, R. D., *Handbook of Powder Technology, Vol 7. Dispersing Powders in Liquids*. Elsevier, Amsterdam, 1988.
- Prabhakaran, K., Narayanan, A. and Pavithran, C., Cardanol as a dispersant plasticizer for an alumina/toluene tape casting slip. *J. Eur. Ceram. Soc.* 2001, **21**, 2873–2878.
- Shanefield, D. J., Physical-chemistry of tape casting. *Abstr. Papers Am. Chem. Soc.* 1986, **191**, 220.
- Kristoffersson, A. and Carlstrom, E., Tape casting of alumina in water with an acrylic latex binder. *J. Eur. Ceram. Soc.* 1996, **17**, 289–297.
- Zeng, Y. P., Jiang, D. L. and Greil, P., Tape casting of aqueous  $Al_2O_3$  slurries. *J. Eur. Ceram. Soc.* 2000, **20**, 1691–1697.
- Reddy, S. B., Singh, P. P., Raghu, N. and Kumar, V., Effect of type of solvent and dispersant on NANO PZT powder dispersion for tape casting slurry. *J. Mater. Sci.* 2002, **37**, 929–934.
- Kleinlogel, C. and Gauckler, L. J., Sintering of nanocrystalline  $CeO_2$  ceramics. *Adv. Mater.* 2001, **13**, 1081–1085.
- Yanez, J., Shikata, T., Lange, F. F. and Pearson, D. S., Shear modulus and yield stress measurements of attractive alumina particle networks in aqueous slurries. *J. Am. Ceram. Soc.* 1996, **79**, 2917–2924.
- Blair, S. C., Berge, P. A. and Berryman, J. G., Using two-point correlation functions to characterize microgeometry and estimate permeabilities of sandstones and porous glass. *J. Geophys. Res.* 1996, **101**, 20359–20375.
- Dardis, O. and McCloskey, J., Permeability porosity relationships from numerical simulations of fluid flow. *Geophys. Res. Lett.* 1998, **25**, 1471–1474.
- Koponen, A., Kataja, M., Timonen, J. and Kandhai, D., Simulations of single-fluid flow in porous media. *Int. J. Modern Phys. C* 1998, **9(8)**, 1505–1521.
- Brinker, C. J. and Scherer, G. W., *Sol–Gel Science: The Physics and Chemistry of Sol–Gel Processing*. Academic Press Inc., Boston, 1999, 319ff.